

Facile Hydrothermal Synthesis of Tellurium Nanostructures for Solar Cells

MokhtarPanahi-Kalamuei, Mehdi Mousavi-Kamazani, Masoud Salavati-Niasari*

Institute of Nano Science and Nano Technology, University of Kashan, Kashan, P. O. Box. 87317-51167, I. R. Iran

Article history:

Article history:

Received 9/10/2014

Accepted 12/11/2014

Published online 21/12/2014

Keywords:

Tellurium

Nanostructure

Thioglycolic acid

Solar cell

**Corresponding author:*

E-mail address:

salavati@kashanu.ac.ir

Phone: +98 3155555 333

Fax: +98 31 5555 29 30

Abstract

Tellurium (Te) nanostructures have been successfully synthesized via a simple hydrothermal method from the reaction of a TeCl_4 aqueous solution with thioglycolic acid (TGA) as a reductant. TGA can be easily oxidized to the corresponding disulfide $[\text{SCH}_2\text{CO}_2\text{H}]_2$, which in turn can reduce TeCl_4 to Te. The obtained Te was characterized by XRD, SEM, EDS, and DRS. The effect of reducing agent on morphology and size of the products were also studied. Additionally, Te thin film was deposited on the FTO- TiO_2 by Dr-blading then employed to solar cell application and measured open circuit voltage (V_{oc}), short circuit current (I_{sc}), and fill factor (FF) were determined as well. The studies showed that particle morphology and sizes play crucial role on solar cell efficiencies.

2014 JNS All rights reserved

1. Introduction

Tellurium (Te) is an interesting p-type semiconductor with direct narrow band gap energy of 0.35 eV at room temperature [1]. It has a wealth of useful properties including nonlinear optical responses, photoconductivity, and thermoelectric properties, which result in their potential applications in electronic and optical electronic devices, piezoelectric devices owing to its non-centrosymmetry, high-efficiency conductors, catalytic activities, carbon monoxide gas sensors and removal of mercury ions [1-5]. Therefore many investigations have been employed for this

substance and various Te nanostructures such as nanotubes, nanowires and nanorods were prepared by different chemical methods such as hydrothermal methods, microwave-assisted synthesis, electrodeposition and physical evaporation method [1-5]. In this paper, we synthesized Te nanostructures by employing simple hydrothermal approach using TeCl_4 as a tellurium precursor and thioglycolic acid (TGA) as a reducing agent. TGA as a 'soft template' controls the morphology and plays a significant role in formation of nanostructures [6, 7]. It can prevent Te nanocrystal aggregation and, in suitable

conditions, can form a complex with Te^{4+} that turns to Te clusters. Additionally, effects of $\text{N}_2\text{H}_4\cdot\text{H}_2\text{O}$ and KBH_4 as reducing agents on morphology and size were studied. A preliminary feasibility study on the developing a solar cell having the fluorine-doped tin oxide (FTO)/ TiO_2 /Te/Pt-FTO structure was also investigated.

2. Experimental

2.1. Materials and physical measurements

All of the chemicals used in the experiments were of analytical grade and used as received without further purification. TeCl_4 , KBH_4 , $\text{N}_2\text{H}_4\cdot\text{H}_2\text{O}$, thioglycolic acid (TGA) and cetyltrimethyl ammonium bromide (CTAB) were purchased from Merck Company. X-ray diffraction (XRD) patterns were recorded by a Philips-X'PertPro, X-ray diffractometer using Ni-filtered $\text{Cu K}\alpha$ radiation at scan range of $10 < 2\theta < 80$. Scanning electron microscopy (SEM) images were obtained on LEO-1455VP equipped with an energy dispersive X-ray spectroscopy. The energy dispersive spectrometry (EDS) analysis was studied by XL30, Philips microscope. The diffused reflectance UV-visible spectrum (DRS) of the sample was recorded by an Ava Spec-2048TEC spectrometer. Photocurrent density-voltage (J-V) curve was measured by using computerized digital multimeters (Ivium-n-Stat Multichannel potentiostat) and a variable load. A 300 W metal xenon lamp (Luzchem) served as assimilated sun light source, and its light intensity (or radiant power) was adjusted to simulated AM 1.5 radiation at 100 mW/cm^2 with a filter for this purpose.

2.2. Preparation of Te nanostructures

In this method 0.05 g of TeCl_4 and 0.05 g of CTAB was dissolved in 35 ml distilled water. Obtained mixture was stirred at room temperature for 5 min. Subsequently, 5 ml of thioglycolic acid (2 M) as reducing agent was added to solution. After 5 min stirring, reagents was loaded into an autoclave (200 ml) and autoclave was kept at $160 \text{ }^\circ\text{C}$ for 10 h and then was allowed to cool down to room temperature naturally. The products was centrifuged and washed with absolute ethanol and distilled water several times and was dried at $70 \text{ }^\circ\text{C}$ for 5 h (sample 1). To study effects of reducing agents, hydrazine hydrate (2 M)(sample 2) and potassium borohydride (sample 3) was used instead of TGA.

2.3. Fabrication of FTO/ TiO_2 /Te/Pt-FTO cell

Electrophoresis deposition (EPD) was utilized to the prepare TiO_2 films [8-10]. During EPD, the cleaned FTO glass remained at a positive potential (anode) while a pure steel mesh was used as the counter (cathode) electrode. The linear distance between the two electrodes was about 3 cm. Power was supplied by a Megatek Programmable DC Power Supply (MP-3005D). The applied voltage was 10 V. The deposition cycle was repeated 4 times, each time 15s, and the temperature of the electrolyte solution was kept constant at $25 \text{ }^\circ\text{C}$. The coated substrates were air dried. The apparent area of the film was $0.5 \times 0.5 \text{ cm}^2$. The obtained layer was annealed under an air flow at $500 \text{ }^\circ\text{C}$ for 30 min. Electrolyte solution and the amount of additives are important for creation a surface with high quality. Based on other experiment reported previously [8-10] we used optimal concentrations of additives in the electrolyte solution as follow: 120 mg/l of I_2 , 48 ml/l of acetone, and 20 ml/l of water. For deposition of Te powder on the FTO glass substrate, a paste of Te was initially prepared.

The slurry was produced by mixing and grinding 1.0 g of the nano-sized Te with ethanol and water in several steps. Afterwards, the ground slurry was sonicated with ultra-sonic horn (Sonicator 3000; bande line, MS 72, Germany), and then mixed with terpineol and ethyl cellulose as binders. After removing the ethanol and water with a rotary-evaporator, the final paste was prepared. The prepared Te paste was coated on TiO₂ film by a doctor blade technique [11]. After that the electrode was gradually heated under an air flow at 450 °C for 30 min. Counter-electrode was made from deposition of a Pt solution on FTO glass. Subsequently, this electrode was placed over TiO₂/Te electrode. Sealing was accomplished by pressing the two electrodes together on a double hot-plate at a temperature of about 110 °C. The redox electrolyte consisting of 0.05 M of LiI, 0.05 M of I₂ and 0.5 M of 4-tert-butylpyridine in acetonitrile as a solvent was introduced into the cell through one of the two small holes drilled in the counter electrode. Finally, these two holes were sealed by a small square of sealing sheet and characterized by I-V test.

3. Results and discussion

The XRD pattern of the as-synthesized Te nanostructures in the presence of TGA (sample 1) is shown in Fig. 1. The diffraction peaks, observed in Fig. 1, can be indexed to pure hexagonal phase of tellurium (space group: P3121) with cell constants $a = b = 4.4579 \text{ \AA}$, $c = 5.9270 \text{ \AA}$ and JCPDS No. 36-1452. The sharp diffraction peaks manifestation shows that the obtained Te nanostructures have high crystallinity. According to XRD data, the crystallite diameter (D_c) of Te nanostructures was calculated to be 17 nm using the Scherer equation (1) [7]:

$$D_c = K\lambda / \beta \cos\theta$$

(1)

Where β is the breadth of the observed diffraction line at its half intensity maximum (101), K is the so-called shape factor, which usually takes a value of about 0.9, and λ is the wavelength of X-ray source used in XRD.

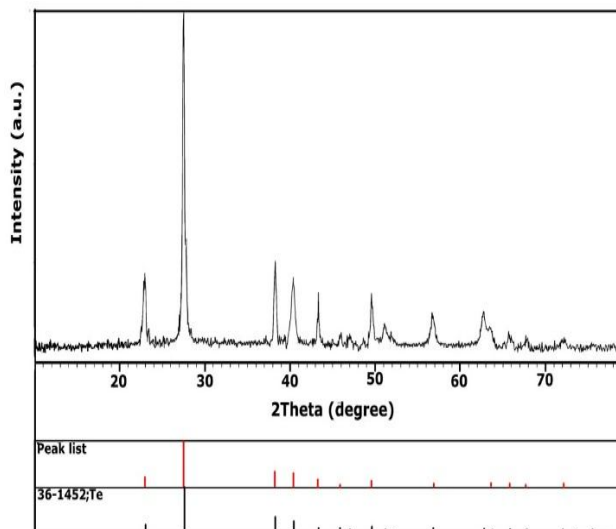


Fig. 1. XRD pattern of the as-synthesized Te nanostructures in the presence of TGA.

EDS analysis was used to investigate the chemical composition and purity of Te nanoparticles (sample 1). The EDS spectrum demonstrates the presence of Te in these nanoparticles (Fig. 2). It is obvious that there is no significant impurity but presence of C and O shows that there may be less organic impurity capped nanoparticles which may arise from CTAB and TGA. Au-peaks is related to the coverage of samples for SEM analysis with this matter. The morphology of products was characterized by SEM. According to SEM images, the obtained products in our experiment are nanoparticles, sheets, rods and microspheres that will be discussed in detail in the following sections.

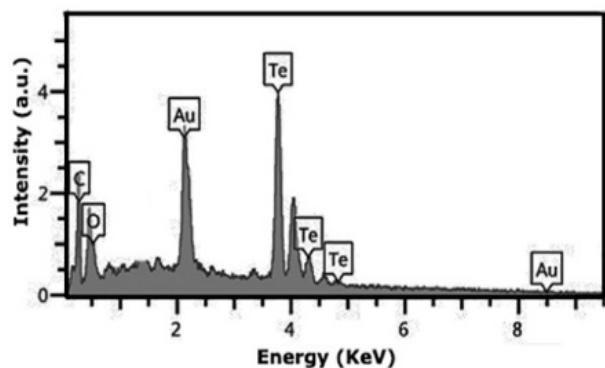


Fig. 2. EDX spectrum of the as-synthesized product via TGA (sample 1).

In order to investigate the reducing agent effect on morphology and particle size, TGA, $N_2H_4.H_2O$ and KBH_4 were used (samples 1-3). Thioglycolic acid as complexing agent plays an important role in the formation of nanostructures [6, 7]. TGA can prevent accumulation of Tenanocrystals and also forms complex with Te^{4+} and finally forms the Te clusters. TGA has $-SH$ and $-COOH$ functional groups [1]. When TGA is used in excess, TGA is adsorbed on the surface of Te nanoparticles and hydrogen and S-S bonds form between them. The S-S and hydrogen bonds of TGA are connected together as a chain and confine the growth of particles and finally form Te nanoparticles. Moreover, during the experiment was found that the under heating TGA, readily oxidized to disulfide and is capable to reduce Te^{4+} to Te. The mechanism of tellurium nanostructures formation in the presence of TGA can be as follow:

$$2HSCH_2CO_2H \rightarrow [SCH_2CO_2H]_2 + H_2(1)$$

$$TeCl_4 + H_2O \rightarrow H_2TeO_3 + 4HCl(2)$$

$$2H_2 + H_2TeO_3 \rightarrow Te + 3H_2O(3)$$

Final reaction: $4HSCH_2CO_2H + H_2TeO_3 \rightarrow [SCH_2CO_2H]_4 + Te + 3H_2O(4)$

So in this experiment, TGA was used as a reducing agent. In other word, by using TGA there is no need

to use of secondary reducing agent for converting Te^{4+} to Te.

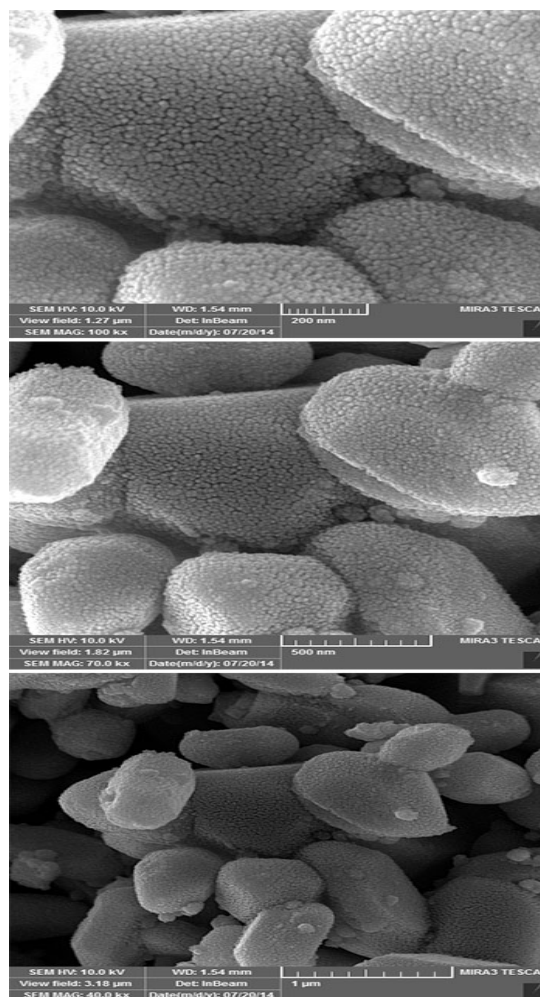
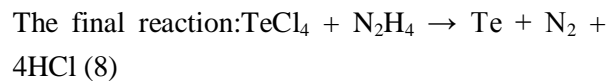
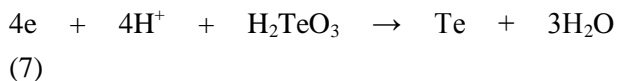


Fig. 3. SEM images of the products in the presence of TGA (sample 1).

When $N_2H_4.H_2O$ was used (sample 2) the morphology changed and sphere-like self-assemblies Te nanostructures was obtained (Fig. 4). Furthermore, the obtained nanoparticles have smaller size and are more homogenous. Mechanism of tellurium nanostructures formation in the presence of hydrazine can be as follow:

$$N_2H_4 \rightarrow N_2 + 4H^+ + 4e(5)$$

$$TeCl_4 + 3H_2O \rightarrow H_2TeO_3 + 4HCl(6)$$



Using KBH_4 (sample 3) morphology also changed and nanoparticles mixed with nanorods and nanospheres were formed (Fig. 5).

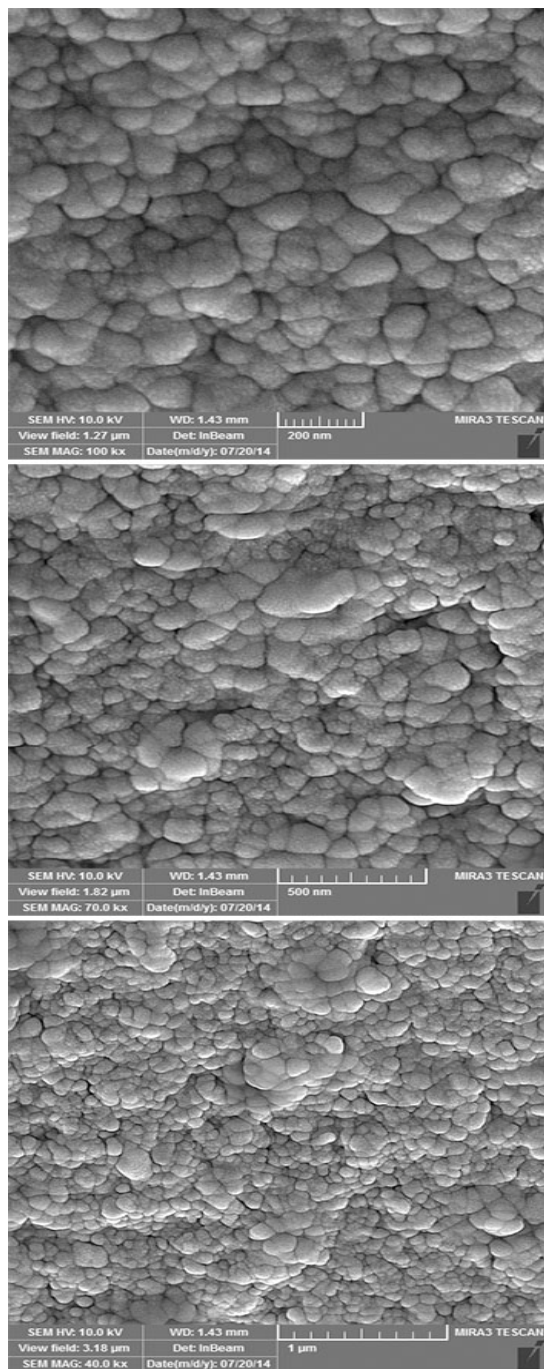


Fig. 4. SEM images of the products in the presence of $N_2H_4.H_2O$ (sample 2).

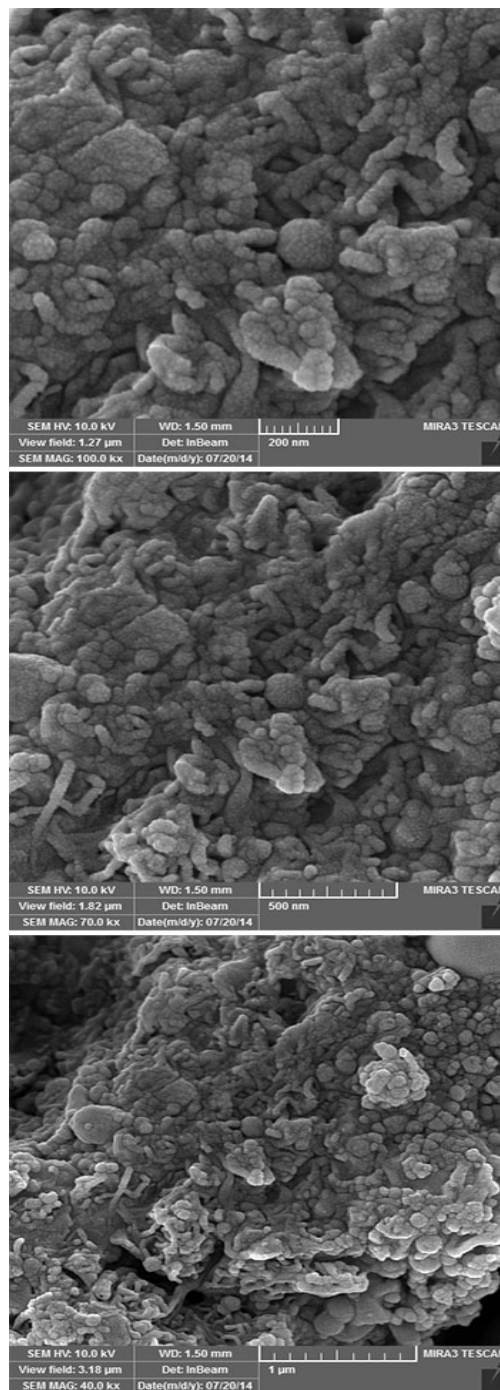
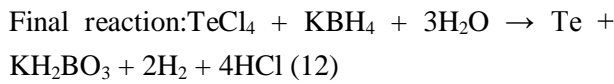
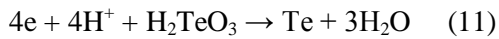
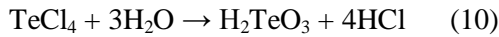


Fig. 5. SEM images of the products in the presence of KBH_4 (sample 3).

Borohydride is stronger reducing agent than TGA and hydrazine, so in the presence of borohydride as a severe reducing agent that increases extremely nucleation rate, the smaller nanoparticles are formed that was agglomerated at some points. The reactions in the presence of KBH_4 can be described as follows:



The UV-Vis absorption spectrum of the as-synthesized Te nanocrystals (sample 1) was recorded as shown in Fig. 6. The absorption edge of obtained Te nanostructures is observed at 581 nm that is in good agreement with the literature [13].

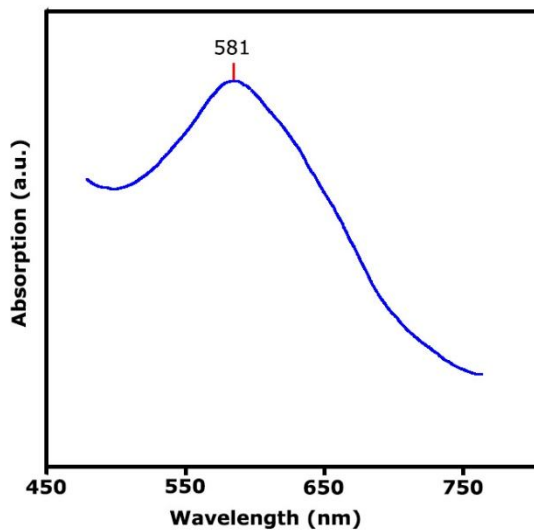


Fig. 6. Diffuse reflectance spectrum of Te nanostructures (sample 1).

Current-voltage characteristic of FTO/ TiO_2 /Te/Pt-FTO cells (Fig. 7) for all samples was studied. The results are listed in the Table 1. As can be seen, different efficiencies are obtained for samples with different shapes and sizes. Stronger electric fields

within bonds result in higher open circuit voltage. To obtain a strong electric field, difference between Fermi levels of two materials (p and n) must be large. For this purpose, semiconductors energy gap must be large. Therefore, open circuit voltage of a solar cell will increase with its energy gap.

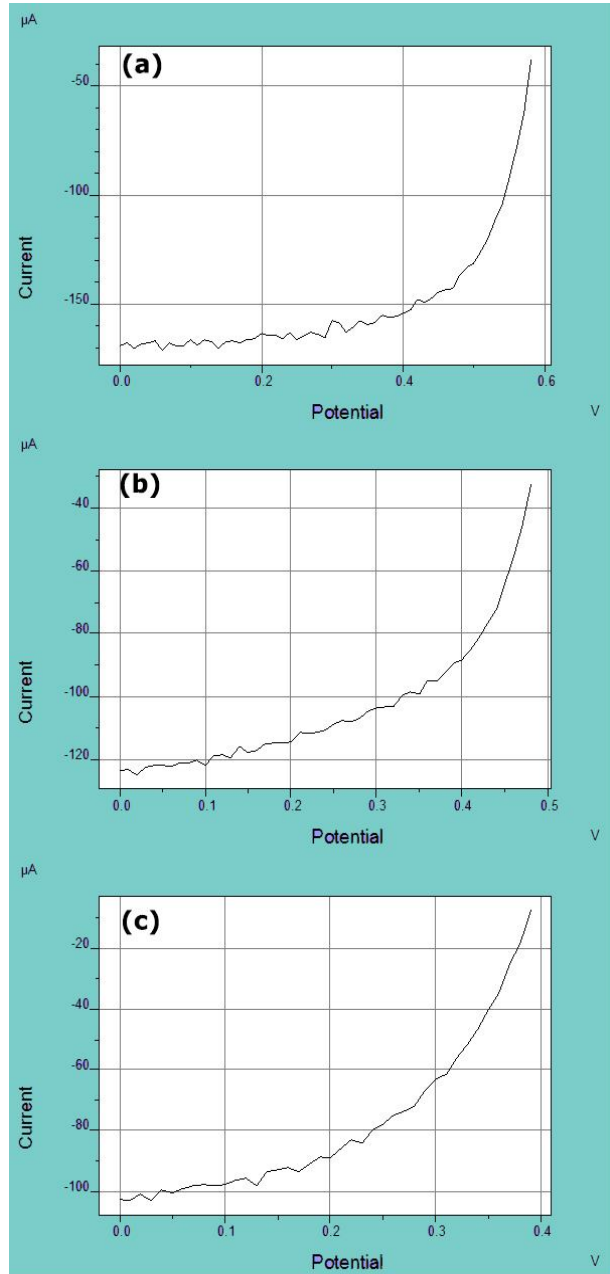


Fig. 7. *J-V* characterization of prepared solar cells a) sample 1, b) sample 2, and c) sample 3.

Although, increasing the energy gap leads to fewer photon could generate electron-hole pairs and as a result, less short-circuit current will be generated. Therefore, increasing energy gap and actually increasing particle size have different effects on open-circuit voltage and short-circuit current. In this respect, an optimal particle size for obtaining high efficiency is offered. Morphology has also effect on efficiency by exposing different surface areas to the light.

Table 1. J-V characteristic of prepared solar cells by Te.

| Sample No | I_{sc} (mA) | J_{sc} (mA/cm ²) | V_{oc} | FF | η (%) |
|-----------|---------------|--------------------------------|----------|------|------------|
| 1 | 0.103 | 0.206 | 0.39 | 0.5 | 0.04 |
| 2 | 0.169 | 0.338 | 0.58 | 0.6 | 0.12 |
| 3 | 0.124 | 0.228 | 0.49 | 0.64 | 0.07 |

4. Conclusion

Summary, Te nanostructures with various shapes have been prepared via a facile hydrothermal route, with thioglycolic acid (TGA) as a new reducing agent for reducing TeCl₄ to Te. In this work, the effect of reducing agent on the morphology and particle size of the products was investigated. To fabricate a FTO/TiO₂/Te/Pt-FTO solar cell, Te film was directly deposited on top of the TiO₂. Solar cell results indicate that there is the possibility of developing an inexpensive solar cell by tellurium produced by this method. The prepared Te products were characterized extensively by means of XRD, EDX, SEM and DRS.

Acknowledgment

Authors are grateful to council of University of Kashan for providing financial support to undertake this work.

References

- [1] M. Panahi-Kalamuei, M. Mousavi-Kamazani, M. Salavati-Niasari, *Mater. Lett.* 136, (2014) 218.
- [2] M. Panahi-Kalamuei, F. Mohandes, M. Mousavi-Kamazani, M. Salavati-Niasari, Z. Fereshteh, M. Fathi, *Mater. Sci. Semicond. Process.* 27, (2014) 1028.
- [3] Y. Wang, Z. Tang, P. Podsiadlo, Y. Elkasabi, J. Lahann, N. Kotov, *Adv. Mater.* 18, (2006) 518.
- [4] S. Sen, K.P. Muthe, N. Joshi, S.C. Gadkari, S.K. Gupta, M. Roy, S.K. Deshpande, J.V. Yakhmi, *Sensor. Actuat. B: Chem.* 98, (2004)154
- [5] R. Zheng, W. Cheng, E. Wang, S. Dong, *Chem. Phys. Lett.* 395, (2004)302.
- [6] M. Panahi-Kalamuei, M. Mousavi-Kamazani, M. Salavati-Niasari, S.M. Hosseinpour-Mashkani, *Ultrason. Sonochem.* 23, (2015)246.
- [7] M. Mousavi-Kamazani, M. Salavati-Niasari, H. Emadi, *Mater. Res. Bull.* 47, (2012)3983.
- [8] M. Mousavi-Kamazani, M. Salavati-Niasari, M. Sadeghinia, *Mater. Lett.* 142, (2015)145.
- [9] M. Panahi-Kalamuei, M. Salavati-Niasari, S.M. Hosseinpour-Mashkani, *J. Alloys Compd.* 617, (2014)627.
- [10] M. Mousavi-Kamazani, M. Salavati-Niasari, *Compos. Part B-ENG.* 56, (2014)490.
- [11] M. Mousavi-Kamazani, M. Salavati-Niasari, M. Ramezani, *J. Clust. Sci.* 24, (2013)927.
- [12] H.H. Li, P. Zhang, C.L. Liang, J. Yang, M. Zhou, X.H. Lu, G.A. Hope, *Cryst. Res. Technol.* 47, (2012)1069.